Electronic Supporting Information

Bioinspired fabrication of optical fiber SPR sensors for immunoassays using polydopamine-accelerated electroless plating

Se Shi,[‡a] Libing Wang,[‡b] Akang Wang,[a] Renliang Huang,[c] Li Ding,[b] Rongxin Su,*[ade] Wei Qi[ade] and Zhimin He[a]

[a]State Key Laboratory of Chemical Engineering, School of Chemical Engineering and Technology, Tianjin University, Tianjin 300072, China

[b]Research Center of Hunan Entry-Exit Inspection and Quarantine Bureau, Changsha, 410001, China

[c]Tianjin Key Laboratory of Indoor Air Environmental Quality Control, School of Environmental Science and Engineering, Tianjin University, Tianjin 300072, China

[d]Collaborative Innovation Center of Chemical Science and Engineering (Tianjin), Tianjin 300072, China

[e]Tianjin Key Laboratory of Membrane Science and Desalination Technology, Tianjin University, Tianjin 300072, China

‡ These authors contributed equally to this work.

*Correspondence and requests for materials should be addressed to R. S. (email: surx@tju.edu.cn)

List of content

1. Analytic methods

1.1 Optical fiber SPR measurement system

Figure S1 shows the schematic diagram of the measurement system using the optical fiber SPR sensor. One end of the sensor was connected to the end of the bifurcated optical fiber (SPLIT-400-VIS-NIR, Ocean Optics), and the other end with the sensing area was immersed into the target solution. The white light emitted from a tungsten-halogen light source (HL-2000-HP, Ocean Optics) was conducted into the sensor through the bifurcated optical fiber. The interaction between the incident light and the sensor was used to modulate the optical signal reflected by the silver layer and captured by a mini-spectrometer (HR4000, Ocean Optics), which was connected to the other end of the bifurcated optical fiber. The signal obtained could be shown and monitored by a computer connected with the spectrometer.

1.2 Scanning electron microscope (SEM)

The thickness of the PDA layer and the surface morphology and thickness of the gold film were characterized using an S-4800 field emission scanning electron microscope (FE-SEM; Hitachi Hightechnologies Co., Japan) at an acceleration voltage of 3 keV.

1.3 Atomic force microscope (AFM)

The surface topography of the PDA surface was characterized using a 5500 atomic force microscope (AFM) equipped with N9797AU-1FP Pico software in contact mode.

2. Supplementary Figures

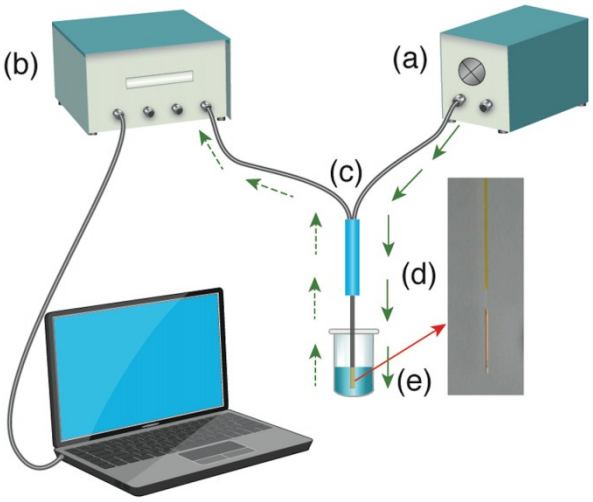

Figure S1 Schematic diagram of the measurement system using the optical fiber SPR sensor. (a) Light source; (b) Spectrometer; (c) Bifurcated optical fiber; (d) Sensor; (e) Target solution.

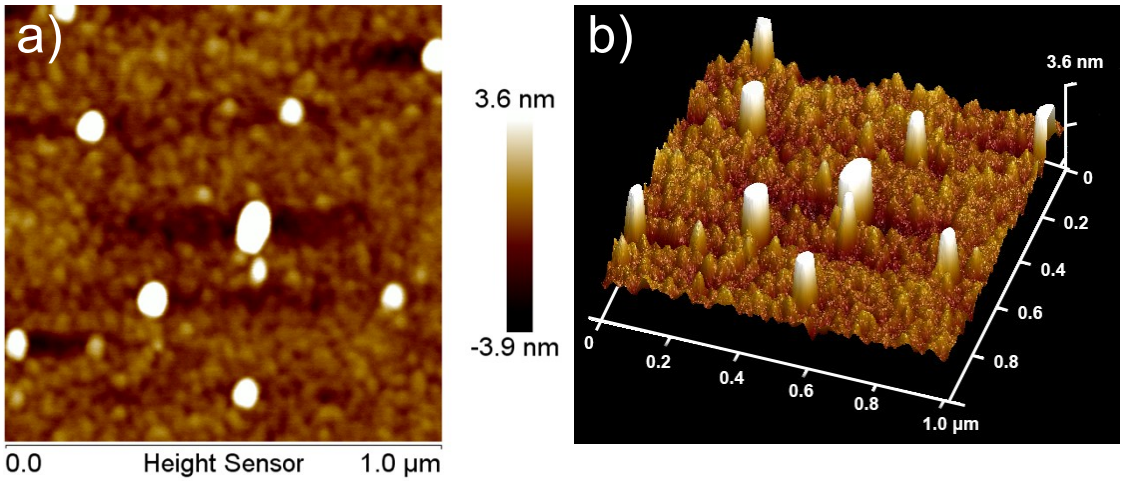

Figure S2 AFM 2D (a) and 3D (b) images of the PDA functionalization layer.

As shown in Fig. S2, the PDA layer had a relatively smooth surface with a surface profile root-mean-square (RMS) roughness of 1.17 nm for the whole area (1 µm × 1 µm). The PDA surface was topographically made up of grains, and few and small nanopores were existed between the grains. These features of PDA surfaces were comparable to those previously reported.[1, 2]

In theory, except the main adsorption on the PDA surface, the gold seeds also could be adsorbed into these pores. However, on the one hand, these nanopores were very small (maximum diameter was about 8 nm), but the gold seeds must grow into large gold nanoparticles (with an about 65 nm

diameter) for the fabrication of SPR sensors. Therefore, the steric hindrance in these small pores may negatively affect the growth of the gold seeds. The relatively higher compactness of the formed PDA layer in this work perhaps was due to the rapid agitation of solution in the polymerization process of dopamine. On the other hand, in this work, the PDA layer had a very smooth surface (RMS roughness was only 1.17 nm), that is to say, the pores was very shallow compared with the thick gold film (about 60 nm) formed in the following electroless plating. Owing to these two reasons, the "penetration into the pores" (as the reported by Zhang et al. [1]) likely has a negligible effect on this work, and it mainly help with the penetration and diffusion of small molecules in the pores of PDA film.

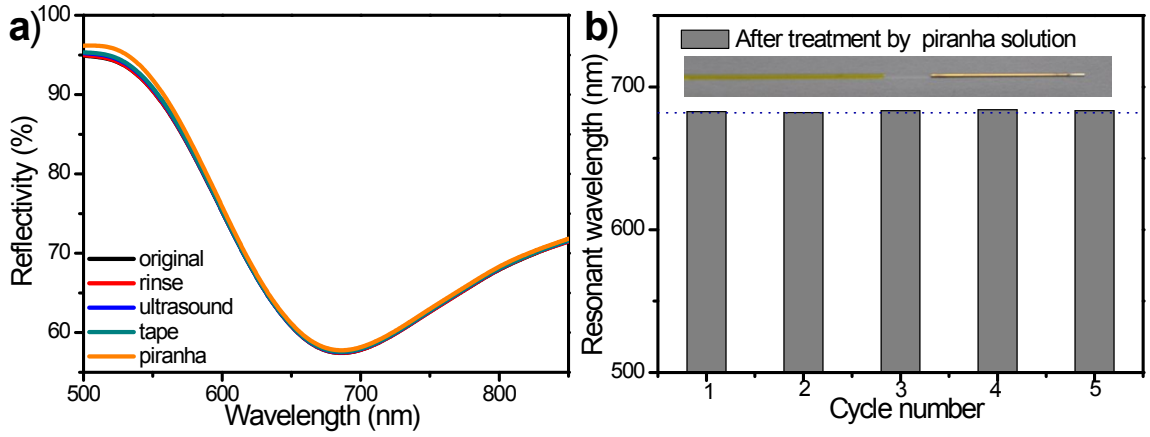

Figure S3 a) Reflectivity spectra of the optical fiber SPR sensor prepared using PDA-accelerated ELP after the following treatment steps: before treatment; rinsing with water and ethanol; ultrasonication in water and ethanol; tape adhesion and immersion in piranha solution. b) Regeneration of the gold film sensors treated by the piranha solution after the immunoassays.

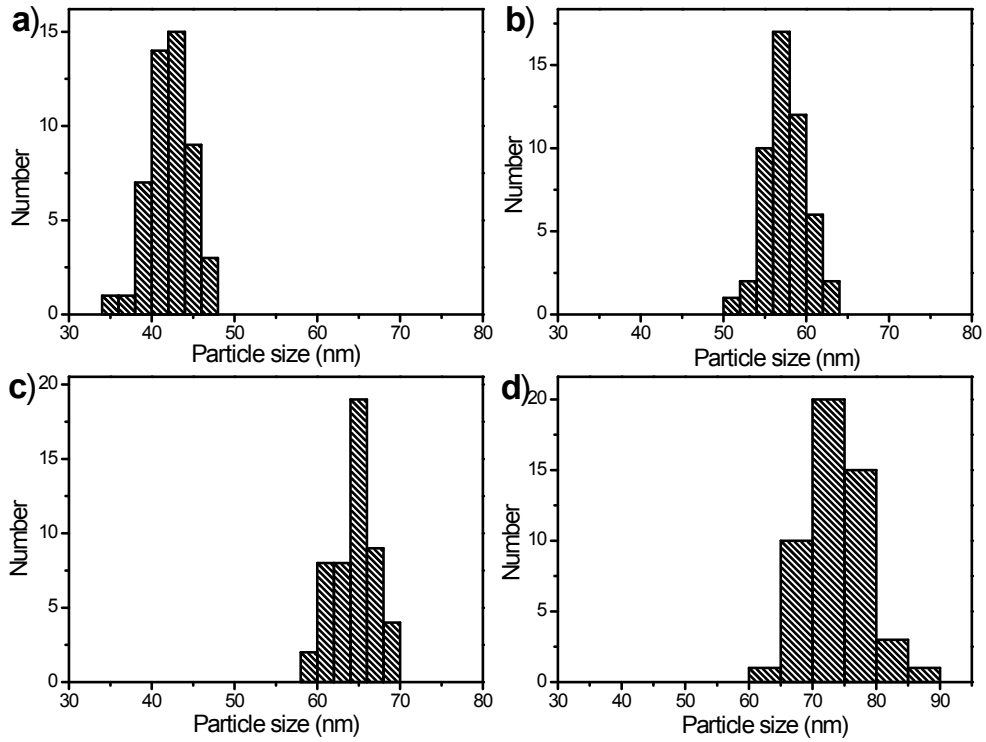

Figure S4 Particle size distributions obtained from SEM images of the surface of sensors prepared with different plating times (a) 4 min, (b) 5 min, (c) 5.5 min and (d) 6 min.

3. Supplementary Tables

Table S1 Refractive index (RI) values of the different solvents used to measure the sensitivity of the prepared sensor to surrounding refractive index change.

Solvent	RI
Methanol	1.328
Water	1.333
Acetonitrile	1.344
Acetone	1.359
Ethanol	1.361
Hexane	1.375
n-Propyl alcohol	1.386

Table S2 Comparison of the refractive index sensitivities of optical fiber SPR sensors prepared by different methods.

Sensor preparation method	Refractive index linear range (RIU)	Sensitivity (nm/RIU)	Reference
Sputtering gold film	1.333-1.347	1557	[3]
	1.333-1.354	1421	[4]
	1.338	1090	[5]
	1.363	2613	
Silver mirror reaction	1.333-1.386	1412-3906	[6]
Traditional ELP	1.333-1.359	2054	[7]
	1.359-1.386	3980	
PDA-accelerated ELP	1.328-1.386	1391-5346	This work
	or 1.333-1.359	2619	
	1.359-1.386	4426	

Table S3 Time comparisons of the substrate functionalization and gold seeds adsorption in the processes of the PDA-accelerated ELP and traditional ELP.

Methods	Applications	Functionalization time	Gold seeds adsorption time	References
Traditional ELP	Prism SPR	12h	16h	[8]
	Optic-fiber SPR	6h	8h	[7]
	Metallization	24h	12-15h	[9]
	Surface coating	overnight	overnight	[10]
PDA-accelerated ELP	Optic-fiber SPR	15 min	2h	This work

Table S4 Resonant wavelength, wavelength shift for the change in the refractive index, and reflectivity values of the sensors fabricated in the same and different batches. Ten sensors were fabricated for one batch.

Batch 1				Batch 2			
Number	Resonant wavelength (nm)	Wavelength shift (nm)	Reflectivity (%)	Number	Resonant wavelength (nm)	Wavelength shift (nm)	Reflectivity (%)
1	682.33	74.07	58.79	1	683.11	74.31	65.39
2	682.68	74.71	67.38	2	681.95	76.87	60.12
3	681.27	76	61.12	3	682.59	75.06	57.71
4	681.26	73.56	60.09	4	683.06	73.34	65.76
5	682.75	73.74	60.71	5	682.94	75.97	62.07
6	681.04	73.78	65.13	6	682.29	76.96	60.06
7	682.11	73.46	63.89	7	683.01	74.49	58.78
8	682.35	76.58	67.69	8	681.19	74.73	60.81
9	682.93	77.2	66.37	9	681.68	76.3	67.35
10	682.28	75.15	64.69	10	682.66	74.38	67.36
[a]CV%	0.09%	1.72%	4.78%	[a]CV%	0.09%	1.54%	5.48%

[a]CV%: Coefficient of variation.

Resonant wavelength: Resonant wavelength of the sensor in the water (RI=1.333); Wavelength shift: Shift of the resonant wavelength of the sensor in ethanol (RI=1.361) compared with that of the sensor in the water.

Table S5 Sensitivity values of the sensors prepared at different DA polymerization temperatures.

Polymerization temperature (°C)	Refractive index linear range (RIU)	Sensitivity (nm/RIU)
4	1.328-1.386	1008-4317
10	1.328-1.386	1391-5346
19	1.328-1.375	1110-4842

Table S6 Sensitivity values of the sensors prepared with different DA polymerization times.

Polymerization time (min)	Refractive index linear range (RIU)	Sensitivity (nm/RIU)
15	1.328-1.386	1391-5346
20	1.328-1.386	1310-4818
25	1.328-1.386	1107-4180

Table S7 Sensitivity values of the sensors prepared with different plating times.

Plating time (min)	Refractive index linear range (RIU)	Sensitivity (nm/RIU)
4	1.328-1.386	868-3242
5	1.328-1.386	837-4371
5.5	1.328-1.386	1391-5346
6	1.328-1.375	1135-5457

Table S8 Comparisons of sensitivity and LOD values of the SPR sensors for the IgG detection.

Sensor	Sensitivity (slope)	Limit of detection (LOD)	Reference
SPR sensors	-	7.11 μg/mL	[11]
	0.40 nm/μg/mL	-	[12]
	0.29 nm/μg/mL	-	[13]
	-	1.00 μg/mL	[14]
	0.33 nm/μg/mL	-	[15]
	0.06-0.33 nm/μg/mL	0.6 μg/mL	[16]
	0.65 nm/μg/mL	0.22 μg/mL	This work

In this work, the sensitivity was defined as the assay response per unit of analyte concentration (the slope of the calibration curve). The limit of detection (LOD) was calculated as the concentration corresponding to the sensor signal that is equal to the mean plus three standard deviations of the background noise.

References

1. W. Zhang, F. K. Yang, Y. Han, R. Gaikwad, Z. Leonenko and B. Zhao, *Biomacromolecules*, 2013, **14**, 394-405.

2. R. A. Zangmeister, T. A. Morris and M. J. Tarlov, *Langmuir*, 2013, **29**, 8619-8628.

3. H. Suzuki, M. Sugimoto, Y. Matsui and J. Kondoh, *Sens. Actuators B: Chem.*, 2008, **132**, 26-33.

4. J. Pollet, F. Delport, K. P. Janssen, K. Jans, G. Maes, H. Pfeiffer, M. Wevers and J. Lammertyn, *Biosens. Bioelectron.*, 2009, **25**, 864-869.

5. Y. Huang, W. Zhang, W. Y. Xie, D. Y. Tang, H. Zhang and C. L. Du, *Sens. Actuators B: Chem.*, 2013, **186**, 199-204.

6. Y. Zhao, Z.-q. Deng and Q. Wang, *Sens. Actuators B: Chem.*, 2014, **192**, 229-233.

7. S. Shi, L. B. Wang, R. X. Su, B. S. Liu, R. L. Huang, W. Qi and Z. M. He, *Biosens. Bioelectron.*, 2015, **74**, 454-460.

8. Y. Lei, H. Chen, H. Dai, Z. Zeng, Y. Lin, F. Zhou and D. Pang, *Biosens. Bioelectron.*, 2008, **23**, 1200-1207.

9. M. A. Raza, H. J. W. Zandvliet, B. Poelsema and E. S. Kooij, *J. Appl. Phys.*, 2013, **113**, 233510.

10. H. Cong, R. Toftegaard, J. Arnbjerg and P. R. Ogilby, *Langmuir*, 2010, **26**, 4188-4195.

11. Y. Liu, Q. Liu, S. Chen, F. Cheng, H. Wang and W. Peng, *Sci. Rep.*, 2015, **5**, 12864.

12. Y. Wang and L. Tang, *Anal. Chim. Acta*, 2013, **796**, 122-129.

13. J. Zhang, Y. Sun, Q. Wu, H. Zhang, Y. Bai and D. Song, *Analyst*, 2013, **138**, 7175-7181.

14. Y. Dong, T. Wilkop, D. Xu, Z. Wang and Q. Cheng, *Anal. Bioanal. Chem.*, 2008, **390**, 1575-1583.

15. G. Manickam, R. Gandhiraman, R. K. Vijayaraghavan, L. Kerr, C. Doyle, D. E. Williams and S. Daniels, *Analyst*, 2012, **137**, 5265-5271.

16. D. Zhang, Y. Sun, Q. Wu, P. Ma, H. Zhang, Y. Wang and D. Song, *Talanta*, 2016, **146**, 364-368.